

Competition between Protein Ligands and Cytoplasmic Inorganic Anions for the Metal Cation: A DFT/CDM Study

Todor Dudev[†] and Carmay Lim^{*,†,‡}

Contribution from the Institute of Biomedical Sciences, Academia Sinica, Taipei 115, and the Department of Chemistry, National Tsing Hua University, Hsinchu 300, Taiwan

Received May 4, 2006; E-mail: carmay@gate.sinica.edu.tw

Abstract: Many of the essential metalloproteins are located in the cell, whose cytoplasmic fluid contains several small inorganic anions, such as Cl^- , NO_2^- , NO_3^- , H_2PO_4^- , and SO_4^{2-} , that play an indispensable role in determining the cell's volume, regulating the cell's pH, signal transduction, muscle contraction, as well as cell growth and metabolism. However, the physical principles governing the competition between these abundant, intracellular anions and protein or nucleic acid residues in binding to cytoplasmic metal cations such as Na^+ , K^+ , Mg^{2+} , and Ca^{2+} are not well understood; hence, we have delineated the physicochemical basis for this competition using density functional theory in conjunction with the continuum dielectric method. The results show that the metal cation can bind to its target protein against a high background concentration of inorganic anions because (i) desolvating a negatively charged Asp/Glu carboxylate in a protein cavity costs much less than desolvating an inorganic anion in aqueous solution and (ii) the metal-binding site acts as a polydentate ligand that uses all its ligating entities to bind the metal cation either directly or indirectly. The results also show that the absolute hydration free energy of the "alien" anion as well as the net charge and relative solvent exposure of the metal-binding protein cavity are the key factors governing the competition between protein and inorganic ligands for a given cytoplasmic metal cation. Increasing the net negative charge of the protein cavity, while decreasing the number of available amide groups for metal binding, protects the metal-bound ligands from being dislodged by cellular anions, thus revealing a "protective" role for carboxylate groups in a protein cavity, in addition to their role in high affinity metal-binding.

Introduction

Because metal ions are essential cofactors in many biologically important proteins, many studies have been carried out to understand the factors governing metal binding and selectivity in metalloproteins. Metal ions have been found to bind generally to a shell of polar hydrophilic residues surrounded by a shell of nonpolar hydrophobic groups in proteins.¹ They tend to bind directly to hydrophilic protein residues, instead of indirectly via a metal-bound water molecule. The metal-binding sites are usually located in relatively buried protein cavities or crevices (characterized by a low dielectric constant), which enhances electrostatic protein ligand–metal interactions, thus favoring the exchange of one or more metal-bound water molecules for protein ligand(s).^{1–3} In most cases, the metal cation binds to a preformed protein pocket whose composition, size, shape, and flexibility play an important role in selecting a given metal cation from the surrounding fluids.^{3–13} As expected, negatively charged

Asp, Glu, and Cys residues are the most common protein ligands found coordinated to the positively charged metal ions.^{14–20} This is because their interactions with the metal cation in a protein cavity are not only thermodynamically favorable, but they are also more favorable than those of other neutral residues or the peptide backbone.^{3,21–25} However, there is an upper limit to the number of negatively charged amino acid residues that may bind

[†] Academia Sinica.

[‡] National Tsing Hua University.

- (1) Yamashita, M. M.; Wesson, L.; Eisenman, G.; Eisenberg, D. *Proc. Natl. Acad. Sci. U.S.A.* **1990**, *87*, 5648–5657.
- (2) Dudev, T.; Lim, C. J. *Phys. Chem. B* **2000**, *104*, 3692–3694.
- (3) Dudev, T.; Lim, C. *Chem. Rev.* **2003**, *103*, 773–787.
- (4) Engeseth, H. R.; McMillin, D. R. *Biochemistry* **1986**, *25*, 2448–2455.
- (5) Falke, J. J.; Snyder, E. E.; Thatcher, K. C.; Voertler, C. S. *Biochemistry* **1991**, *30*, 8690–8697.
- (6) Drake, S. K.; Zimmer, M. A.; Kundrot, C.; Falke, J. J. *J. Gen. Physiol.* **1997**, *110*, 173–184.
- (7) Garmer, D. R.; Gresh, N.; Roques, B.-P. *Proteins* **1998**, *31*, 42–60.

- (8) Hunt, J. A.; Ahmed, M.; Fierke, C. A. *Biochemistry* **1999**, *38*, 9054–9062.
- (9) Huang, D. T. C.; Thomas, M. A. W.; Christopherson, R. I. *Biochemistry* **1999**, *38*, 9964–9970.
- (10) Lee, L. V.; Poyner, R. R.; Vu, M. V.; Cleland, W. W. *Biochemistry* **2000**, *39*, 4821–4830.
- (11) Cox, E. H.; Hunt, J. A.; Compher, K. M.; Fierke, C. A.; Christianson, D. W. *Biochemistry* **2000**, *39*, 13687–13694.
- (12) Babu, C. S.; Dudev, T.; Casareno, R.; Cowan, J. A.; Lim, C. J. *Am. Chem. Soc.* **2003**, *125*, 9318–9328.
- (13) Dudev, T.; Lim, C. J. *Phys. Chem. B* **2001**, *105*, 4446–4452.
- (14) Carrell, C. J.; Carrell, H. L.; Erlebach, J.; Glusker, J. P. *J. Am. Chem. Soc.* **1988**, *110*, 8651–8656.
- (15) Jernigan, R.; Raghunathan, G.; Bahar, I. *Curr. Opin. Struct. Biol.* **1994**, *4*, 256–263.
- (16) Rulisek, L.; Vondrasek, J. J. *Inorg. Biochem.* **1998**, *71*, 115–127.
- (17) Dudev, T.; Cowan, J. A.; Lim, C. J. *Am. Chem. Soc.* **1999**, *121*, 7665–7673.
- (18) Harding, M. M. *Acta Crystallogr.* **2001**, *D57*, 401–411.
- (19) Dudev, T.; Lim, C. J. *Am. Chem. Soc.* **2006**, *128*, 1553–1561.
- (20) Dudev, T.; Lin, Y. L.; Dudev, M.; Lim, C. J. *Am. Chem. Soc.* **2003**, *125*, 3168–3180.
- (21) Garmer, D. R.; Gresh, N. J. *Am. Chem. Soc.* **1994**, *116*, 3556–3567.
- (22) Mercero, J. M.; Fowler, J. E.; Ugalde, J. M. *J. Phys. Chem. A* **2000**, *104*, 7053–7060.
- (23) Rulisek, L.; Havlas, Z. *J. Am. Chem. Soc.* **2000**, *122*, 10428–10439.
- (24) Rulisek, L.; Havlas, Z. *J. Phys. Chem. A* **2002**, *106*, 3855–3866.
- (25) Mercero, J. M.; Matxain, J. M.; Lopez, X.; Fowler, J. E.; Ugalde, J. M. *Int. J. Quantum Chem.* **2002**, *90*, 859–881.

a metal cation of charge q — this limit has been shown to be $q + 2$ by recent calculations.¹⁹ Among the noncharged residues flanking the metal-binding sites, His, Asn, and Gln side chains, and backbone peptide groups are the most abundant.^{15–18,20}

Many of the essential metalloproteins are located in the cell, whose cytoplasmic fluid contains several small inorganic anions such as Cl^- , NO_2^- , NO_3^- , H_2PO_4^- , and SO_4^{2-} . These anions play an indispensable role in physiological processes such as cell volume regulation, signal transduction, muscle contraction, as well as cell growth and metabolism.^{26–28} The intracellular concentration of inorganic anions, which varies with the type and function of the cell, is relatively high: it ranges from 0.1 mM for SO_4^{2-} ,²⁹ to 3–12 mM for NO_3^- ,^{27,30} 5–10 mM for H_2PO_4^- ,^{26,31} and 5–20 mM for Cl^- .²⁸ Thus, these abundant, inorganic anions in the intracellular fluids could compete with protein and nucleic acid residues for binding to cytoplasmic metal cations such as Na^+ , K^+ , Mg^{2+} , and Ca^{2+} . This raises the following intriguing questions: (1) How could the metal cation bind to its target protein against such a high background concentration of inorganic anions? In other words, why does the metal ion prefer binding to its target protein rather than cellular anions? (2) What are the factors governing the competition between protein and inorganic ligands for a given cytoplasmic metal cation? (3) Once the metal cation is bound to the protein ligands, how does the metal-binding site defend itself from alien attack by cellular anions that may disrupt the native binding-site geometry? In particular, for a dication such as Mg^{2+} (that is typically bound to one or two acidic side chains, a few amide groups, and water molecules) would it exchange one of its neutral ligands for a negatively charged inorganic ion given that a dication could bind as many as four negatively charged ligands (see above)? There appear to be no systematic studies addressing these questions (to the best of our knowledge), although studies addressing the competition between protein ligands and water molecules (as opposed to cellular anions) for a given metal cation have been performed.^{3,12,21,24,32–42}

Herein, our goal is to address the above questions and delineate the physicochemical basis governing the competition between protein ligands and cellular anions for the metal cation. Specifically, we assess the role of (i) the dielectric medium, (ii) the composition and net charge of the protein binding pocket, and (iii) the size, charge, and binding mode (mono vs bidentate)

of the inorganic anion in the competitive binding to the metal cation. Chloride, phosphate, and sulfate were chosen as representatives of the inorganic anions because they are among the most common anionic species found in the intracellular space. Furthermore, they possess distinct ligating properties, thus allowing us to assess the effects of varying anion size, charge, and binding mode. Mg^{2+} -binding sites were chosen as model systems in our study because Mg^{2+} -containing proteins play an important role in many enzymatic reactions in the cell, and are well studied both experimentally and theoretically.^{3,12,17,19,20,32,33,43–47} Furthermore, Mg^{2+} is one of the most abundant metal dications in the intracellular medium⁴⁴ and is predominantly hexacoordinated in proteins,^{15,48} unlike Ca^{2+} , whose CN in proteins and in solution appears to be more variable. We used density functional theory (DFT) in conjunction with the continuum dielectric method (CDM) to compute the free energies of exchanging a Mg^{2+} -bound ligand (water or carboxylate side chain or backbone peptide group) with an inorganic cellular anion in sites of varying solvent exposure. The theoretical conclusions are supported by findings from a PDB survey of Mg^{2+} -binding sites containing inorganic anions bound to the metal ion.

Methods

Models Used. Although phosphate and sulfate could exist in more than one ionization state, our focus is on the most likely charge state at physiological pH. Because of the low pK_2 of H_2SO_4 ($= 2^{49}$), dianionic sulfate, SO_4^{2-} , is the sole sulfate species at physiological pH. As the pK_1 , pK_2 , and pK_3 values for the dissociation of H_3PO_4 into H_2PO_4^- , HPO_4^{2-} , and PO_4^{3-} are 2.2, 7.2, and 12.3, respectively,⁴⁹ monoanionic H_2PO_4^- was considered to be the dominant phosphate species at ambient pH.

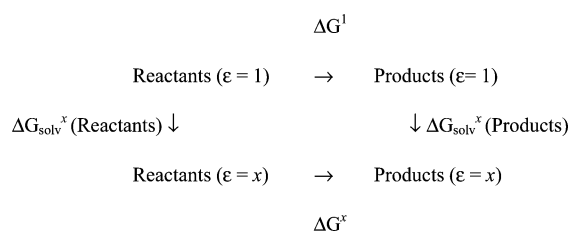
Two types of typical Mg^{2+} -binding sites¹⁷ were considered: the type 1 sites consist of one deprotonated acidic side chain (Asp or Glu) and two neutral residues (Asn/Gln side chains or backbone peptide groups), while type 2 sites comprise two carboxylates and one neutral residue. The protein ligands were modeled as polydentate ligands, where the ligating groups ($-\text{COO}^-$ and $-\text{CONH}_2$) are separated by a minimum number of flexible polymethylene spacers $-(\text{CH}_2)_n-$ ($n = 5, 6$), which would impose no additional strain upon complexation with the metal cation. Those in type 1 Mg^{2+} -binding sites, were modeled by $^-\text{OOC}-(\text{CH}_2)_6-\text{CH}(\text{CONH}_2)-(\text{CH}_2)_5-\text{CONH}_2$ (referred to as **a–b–b**), while those in type 2 Mg^{2+} -binding sites, were modeled by $^-\text{OOC}-(\text{CH}_2)_6-\text{CH}(\text{CONH}_2)-(\text{CH}_2)_5-\text{COO}^-$ (referred to as **a–b–a**). As Mg^{2+} is experimentally determined to be hexahydrated in aqueous solution and is found predominantly hexacoordinated in proteins,^{15,48} hexacoordinated Mg^{2+} complexes were modeled in this study.

DFT Calculations. Geometries. Full geometry optimization for each complex studied was carried out using the Gaussian 03 program⁵⁰ employing the S-VWN functional and the 6-31+G* basis set. This functional/basis set combination was chosen as it reproduces the experimentally observed metal–ligand bond distances in a number of metal–ligand complexes within experimental error.¹⁹ For each fully optimized structure, S-VWN/6-31+G* vibrational frequencies were computed to verify that the molecule was at the minimum of its potential energy surface. No imaginary frequency was found in any of the metal complexes.

- (26) Schachtman, D. P.; Reid, R. J.; Ayling, S. M. *Plant Physiol.* **1998**, *116*, 447–453.
- (27) Crawford, N. M.; Glass, A. D. M. *Trends Plant Sci.* **1998**, *3*, 389–395.
- (28) Akabas, M. H.; Chloride channels. In *Encyclopedia of Life Sciences*, Nature Publishing Group: 2001; pp 1–7.
- (29) Dreyfuss, J.; Pardee, A. B. *J. Bacteriol.* **1966**, *91*, 2275–2280.
- (30) Cruz, L.; Moroz, L. L.; Gillette, R.; Sweedler, J. V. *J. Neurochem.* **1997**, *69*, 110–115.
- (31) Rebeille, F.; Bligny, R.; Douce, R. *Plant. Physiol.* **1984**, *1984*, 355–359.
- (32) Kluge, S.; Weston, J. *Biochemistry* **2005**, *44*, 4877–4885.
- (33) Gresh, N.; Garmer, D. R. *J. Comput. Chem.* **1996**, *17*, 1481–1495.
- (34) Cini, R.; Musaev, D. G.; Marzilli, L. G.; Morokuma, K. *Theochem.* **1997**, *392*, 55.
- (35) Bock, C. W.; Katz, A. K.; Markham, G. D.; Glusker, J. P. *J. Am. Chem. Soc.* **1999**, *121*, 7360–7372.
- (36) Tiraboschi, G.; Roques, B.-P.; Gresh, N. *J. Comput. Chem.* **1999**, *20*, 1379–1390.
- (37) Tiraboschi, G.; Gresh, N.; Giessner-Prettre, C.; Pedersen, L. G.; Deerfield, D. W. *J. Comput. Chem.* **2000**, *21*, 1011–1039.
- (38) Rulisek, L.; Havlas, Z. *J. Am. Chem. Soc.* **2000**, *122*, 10428–10439.
- (39) Gresh, N.; Polcar, C.; Giessner-Prettre, C. *J. Phys. Chem. A* **2002**, *106*, 5660–5670.
- (40) Rulisek, L.; Havlas, Z. *J. Phys. Chem. B* **2003**, *107*, 2376–2385.
- (41) Mercero, J. M.; Matxain, J. M.; Rezabal, E.; Lopez, X.; Ugalde, J. M. *Int. J. Quantum Chem.* **2004**, *98*, 409–424.
- (42) Rezabal, E.; Mercero, J. M.; Lopez, X.; Ugalde, J. M. *J. Inorg. Biochem.* **2006**, *100*, 374–384.

- (43) Black, C. B.; Cowan, J. A. *Inorg. Chem.* **1994**, *33*, 5805–5808.
- (44) Cowan, J. A. *Biological Chemistry of Magnesium*. VCH: New York, 1995.
- (45) Cowan, J. A. *Chem. Rev.* **1998**, *98*, 1067–1087.
- (46) Dudev, T.; Lim, C. J. *Phys. Chem. B* **2004**, *108*, 4546–4557.
- (47) Dudev, T.; Chang, L.-Y.; Lim, C. J. *Am. Chem. Soc.* **2005**, *127*, 4091–4103.
- (48) Marcus, Y. *Chem. Rev.* **1988**, *88*, 1475–1498.
- (49) Weast, R. C. *CRC Handbook of Chemistry and Physics*. CRC: West Palm Beach, FL, 1978.
- (50) Frisch, M. J. et al. *Gaussian 03, rev. B.03*, Gaussian, Inc.: Pittsburgh, PA, 2003.

Scheme 1



Gas-Phase Free Energies. On the basis of the fully optimized S-VWN/6-31+G* geometries, the electronic energies, E_{elec} , were evaluated using the B3-LYP functional in conjunction with the large 6-311++G(2df,2p) basis set. The latter was chosen from among several other basis sets as the gas-phase formation energy of $[\text{Mg}(\text{H}_2\text{O})_6]^{2+}$ was found to converge at this level of theory (see Supporting Information Table 1). The thermal energy, including zero-point energy (E_{T}), work (PV) and entropy (S) corrections were evaluated using standard statistical mechanical formulas⁵¹ where the S-VWN/6-31+G* frequencies were scaled by an empirical factor of 0.9833.⁵² The differences ΔE_{elec} , ΔE_{T} , ΔPV , and ΔS between the products and reactants were used to compute the reaction free energy in the gas phase at room temperature, $T = 298.15$ K, according to the following expression:

$$\Delta G^1 = \Delta E_{\text{elec}} + \Delta E_{\text{T}} + \Delta PV - T\Delta S \quad (1)$$

Continuum Dielectric Calculations. The free energy in a given environment characterized by a dielectric constant $\epsilon = x$ was calculated according to Scheme 1. ΔG^1 , the gas-phase free energy, was computed using eq 1, as described above. ΔG_{sol}^x , the free energy for transferring a molecule in the gas phase to a continuous solvent medium characterized by a dielectric constant, x , was estimated by solving Poisson's equation using finite difference methods.^{53,54} Thus, the reaction free energy in an environment modeled by dielectric constant x , ΔG^x , can be computed from:

$$\Delta G^x = \Delta G^1 + \Delta G_{\text{sol}}^x(\text{products}) - \Delta G_{\text{sol}}^x(\text{reactants}) \quad (2)$$

The solvation free energies were evaluated using the MEAD program.⁵⁵ Details of the Poisson calculations and the *effective* solute radii, which were obtained by adjusting the CHARMM (version 22)⁵⁶ van der Waals radii to reproduce the experimental hydration free energies of the metal cations and ligands, are given in Supporting Information. The calculated hydration free energies of Mg^{2+} , H_2O , HCONH_2 , Cl^- , CH_3COO^- , H_2PO_4^- , and SO_4^{2-} are within 1 kcal/mol of the respective experimental values (Supporting Information, Table 2).

Database Survey. The Protein Data Bank⁵⁷ was surveyed for ≤ 2.0 Å X-ray and NMR structures of proteins containing Mg^{2+} which is bound not only to water and amino acid ligands but also to chloride, phosphate, or sulfate. Polynuclear metal-binding sites or those containing other ligands, such as ATP and ADP, were excluded from the survey. If two or more Mg^{2+} -binding sites have the same composition, only one representative structure, namely, that solved at the highest resolution, was included in the survey.

Results

Competition Between Cellular Ions and Water Molecules for Mg^{2+} in Solution.

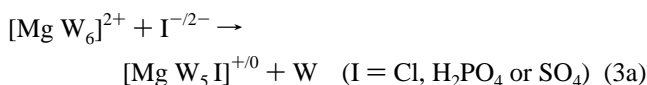
Before Mg^{2+} reaches a protein cavity,

Table 1. Calculated Enthalpies (ΔH^1), Entropic Terms ($T\Delta S^1$), Gas-Phase (ΔG^1) and Solution (ΔG^{80}) Free Energies for Exchanging a Mg^{2+} -Bound Water Molecule (W) with an Inorganic Anion (I) in $[\text{Mg W}_6]^{2+}$ Complexes (in kcal/mol)^a

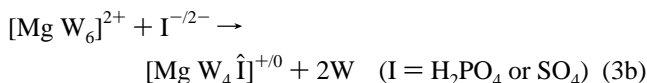
$[\text{Mg W}_6]^{2+} + \text{I}$	product + W	ΔH^1	$T\Delta S^1$	ΔG^1	ΔG^{80b}
Cl^-	$[\text{Mg W}_5 \text{Cl}]^+$	-182.3	3.4	-185.7	11.7
H_2PO_4^-	$[\text{Mg W}_5 (\text{H}_2\text{PO}_4)]^+$	-193.6	-2.4	-191.2	10.1
H_2PO_4^-	$[\text{Mg W}_4 (\text{H}_2\text{PO}_4)]^+ + \text{W}$	-174.4	9.0	-183.4	11.7
SO_4^{2-}	$[\text{Mg W}_5 (\text{SO}_4)]^0$	-376.7	-4.4	-372.2	40.2
SO_4^{2-}	$[\text{Mg W}_4 (\text{SO}_4)]^0 + \text{W}$	-369.7	8.2	-377.9	27.6

^a $\text{H}_2\text{P}\hat{\text{O}}_4$ and $\text{S}\hat{\text{O}}_4$ denote that two of the oxygen atoms are bound to the metal ion. ^b Calculated using the experimental $\Delta G_{\text{sol}}^{80}$ values for H_2O (-6.3 kcal/mol⁵⁹), Cl^- (-75.8 kcal/mol⁶⁰), H_2PO_4^- (-104.3 kcal/mol), and SO_4^{2-} (-247.9 kcal/mol).

could the metal ion be trapped by anions in the cell; i.e., could cellular anions such as Cl^- , H_2PO_4^- , and SO_4^{2-} bind to Mg^{2+} by displacing a metal-bound water molecule? To answer this question, we modeled the exchange of a Mg^{2+} -bound water molecule, W, for an inorganic anion, I, in the aqueous cellular environment ($\epsilon = 80$). Two cases were considered: (i) when the inorganic ion I binds to the metal cation *monodentately* (via one of the oxygen atoms in the case of the oxyanions), i.e.



and (ii) when the oxyanion binds to the metal ion *bidentately* (via two oxygen atoms), i.e.



In eq 3b, $\hat{\text{I}}$ denotes dihydrogen phosphate or sulfate bidentately bound to Mg^{2+} . As a search for X-ray structures in the Cambridge Structure Database (CSD)⁵⁸ for Mg^{2+} bound to a negatively charged ligand shows Mg^{2+} hexacoordinated to five water molecules and a nitrate (CSD entry JAWQON), phenoxyacetate (entry BIZYIS), or propionate derivative (entry IDARIO), Mg^{2+} is assumed to remain hexacoordinated upon water \rightarrow anion exchange. The enthalpies, entropies, and free energies evaluated for eq 3 are listed in Table 1. Structures of the fully optimized $[\text{Mg W}_5 \text{I}]^{+/0}$ and $[\text{Mg W}_4 \hat{\text{I}}]^{+/0}$ complexes ($\text{I} = \text{Cl}, \text{H}_2\text{PO}_4$, or SO_4) are shown in Supporting Information Figure 1.

The results in Table 1 show that whether a metal-bound water molecule could be displaced by an inorganic anion strongly depends on the dielectric medium but not on the binding mode of an oxyanion. In the gas phase, attack of an inorganic anion to the $[\text{Mg W}_6]^{2+}$ dication is enthalpically driven and highly favorable in all cases, as evidenced by the large negative ΔH^1 and ΔG^1 values in Table 1. This is due to the attractive electrostatic interactions between the oppositely charged ionic reactants, which also accounts for the more favorable water–dianion exchange (Table 1, reactions 4 and 5), as compared to the respective water–monoanion substitution (Table 1, reactions 1–3) in the gas phase. Solvation effects, however, reverse these trends in solution. The large desolvation penalties for the reactants (76, 104, 248, and 208 kcal/mol for Cl^- , H_2PO_4^- , SO_4^{2-} , and $[\text{Mg W}_6]^{2+}$, respectively) outweigh the corresponding gas-phase free energy gain, making the water \rightarrow anion exchange unfavorable in aqueous solution (Table 1, positive

- (51) McQuarrie, D. A. *Statistical Mechanics*. Harper and Row: New York, 1976.
 (52) Wong, M. W. *Chem. Phys. Lett.* **1996**, 256, 391–399.
 (53) Gilson, M. K.; Honig, B. *Biopolymers* **1986**, 25, 2097–2119.
 (54) Lim, C.; Bashford, D.; Karplus, M. *J. Phys. Chem.* **1991**, 95, 5610–5620.
 (55) Bashford, D., An object oriented programming suite for electrostatic effects in biological molecules. In *Scientific Computing in Object-Oriented Parallel Environments*, Ishikawa, Y.; Oldehoeft, R. R.; Reynders, V. W.; Tholburn, M., Eds. Springer: Berlin, 1997; Vol. 1343, pp 233–240.
 (56) Brooks, B. R.; Brucoleri, R. E.; Olafson, B. D.; States, D. J.; Swaminathan, S.; Karplus, M. *J. Comput. Chem.* **1983**, 4, 187–217.
 (57) Bernstein, F. C.; Koetzle, T. F.; Williams, G. J. B.; Meyer, E. F.; Brice, M. D.; Rodgers, J. R.; Kennard, O.; Shimanouchi, T.; Tasumi, M. *J. Mol. Biol.* **1977**, 122, 535–542.

(58) Allen, F. H. *Acta Crystallogr.* **2002**, B58, 380–388.

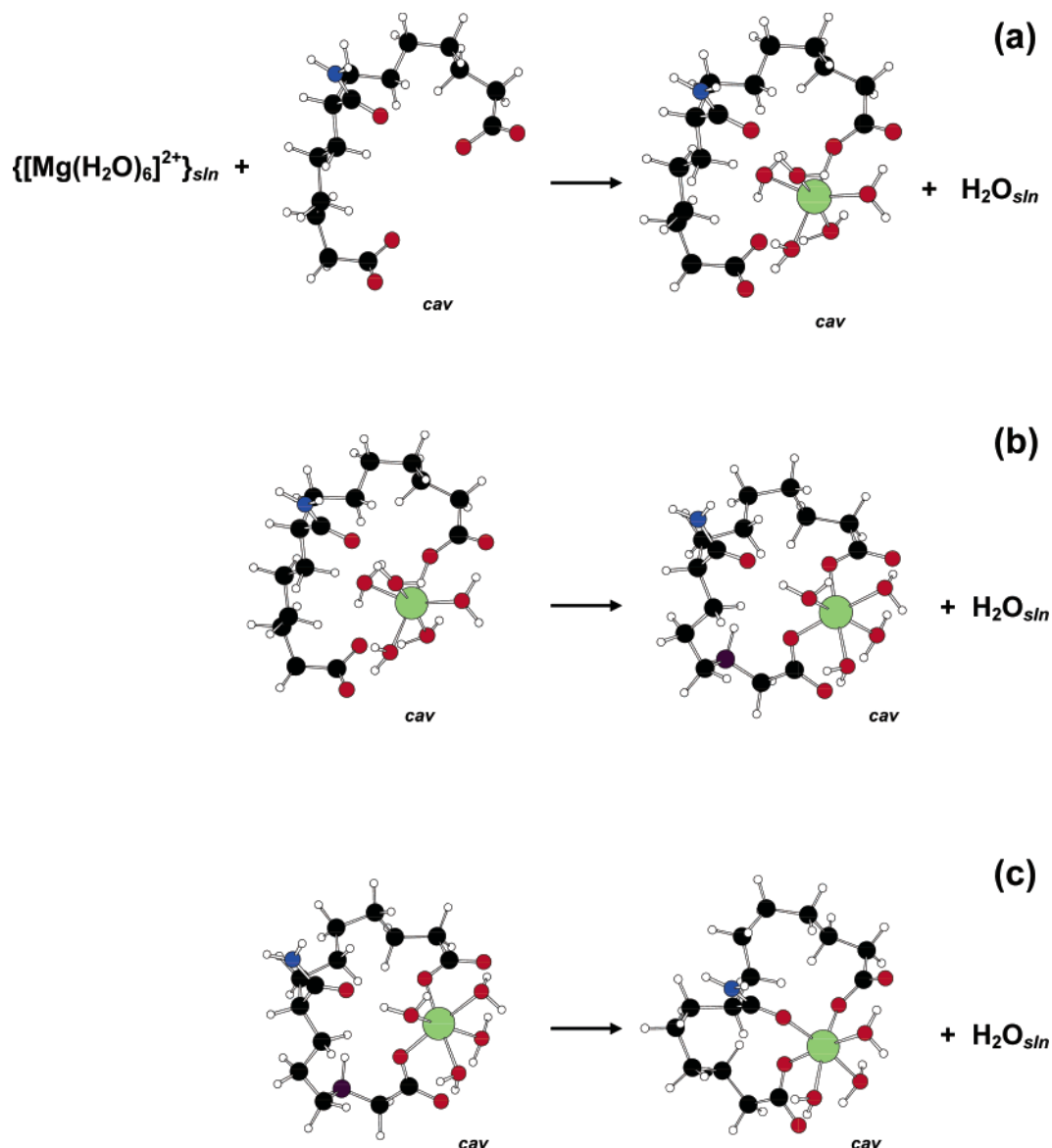


Figure 1. Schematic representation of stepwise binding of Mg^{2+} to a protein cavity $^-\text{OOC}-(\text{CH}_2)_6-\text{CH}(\text{CONH}_2)-(\text{CH}_2)_5-\text{COO}^-$ (a–b–a). The subscript “cav” indicates a protein cavity, while the subscript “sln” denotes aqueous solution.

ΔG^{80}). Moreover, the water $\rightarrow \text{SO}_4^{2-}$ exchange reactions are more unfavorable than the respective water \rightarrow monoanion substitutions (Table 1, ΔG^{80} for the last two reactions are more positive than those for the other reactions) due to the much greater cost of desolvating dianionic SO_4^{2-} , as compared to monoanionic Cl^- and H_2PO_4^- (see above). The monodentate vs bidentate binding mode of the oxyanions does *not* affect the thermodynamic outcome of the water \rightarrow anion exchange in the gas phase or in solution (Table 1, compare reactions 2 with 3, and 4 with 5).

In conclusion, the results in Table 1 imply that inner-shell binding of cellular inorganic anions to Mg^{2+} in aqueous solution is thermodynamically unlikely because of the high cost of desolvating these anions in aqueous solution.

Mg^{2+} Binding to a Protein Cavity. Having shown that Mg^{2+} would not be trapped by anions in the cell, the next step is to model the substitution of the metal-bound water molecules by amino acid residues lining a protein cavity, taking into account the change in the dielectric environment of the incoming/outgoing species. The initial exchange of the *first* Mg^{2+} -bound

water molecule for a protein ligand can be decomposed into three steps: (1) desolvation of the Mg^{2+} cation in coming from bulk solution ($\epsilon = 80$) to a protein cavity characterized by a dielectric constant, $\epsilon = 2, 4, 10$, or 20 ; (2) exchange of a Mg^{2+} -bound water molecule for a carboxylate side chain rather than a carbonyl group, which would be electrostatically less favorable; and (3) release of the liberated water molecule from the metal-binding site ($\epsilon = 2, 4, 10$, or 20) into bulk solution ($\epsilon = 80$). These three steps can be represented by the single reaction depicted in Figure 1a, where the subscript “cav” indicates a protein cavity and the subscript “sln” denotes aqueous solution. The subsequent substitutions of the *second* and *third* Mg^{2+} -bound water molecules for protein ligands (carboxylic or amide groups) occur inside the protein cavity (denoted by b and c of Figure 1), with the displaced water molecules released into bulk solution.

Following the scheme shown in Figure 1, the thermodynamic parameters for the stepwise binding of Mg^{2+} to the two model protein ligands, (a–b–b) $^-$ and (a–b–a) $^{2-}$ (see Methods, **Models Used** subsection), in a preformed rigid protein cavity

Table 2. Calculated Enthalpies, ΔH^\dagger , Entropic Terms, $T\Delta S^\dagger$, and Free Energies, ΔG^x ($x = 1, 2, 4, 10$, or 20) for Exchanging a Mg^{2+} -Bound Water Molecule (W) with a Protein Ligand (L = a–b–b or a–b–a) in Mg^{2+} Complexes (in kcal/mol)^a

Reactants	Product + W	ΔH^\dagger	$T\Delta S^\dagger$	ΔG^1	ΔG^2	ΔG^4	ΔG^{10}	ΔG^{20}
1. $[\text{Mg W}_6]^{2+} + (\text{a-b-b})^-$	$[\text{Mg W}_5 (\text{A-b-b})]^+$			–246.3 ^b	–32.6	–23.5	–16.0	–13.1
2. $[\text{Mg W}_5 (\text{A-b-b})]^+$	$[\text{Mg W}_4 (\text{A-B-b})]^+$	6.3	10.4	–4.1	–9.7	–9.0	–8.2	–7.8
3. $[\text{Mg W}_5 (\text{A-b-b})]^+$	$[\text{Mg W}_4 (\text{A-b-B})]^+$	5.4	11.6	–6.2	–11.6	–11.0	–10.5	–10.2
4. $[\text{Mg W}_4 (\text{A-b-B})]^+$	$[\text{Mg W}_3 (\text{A-B-B})]^+$	7.7	10.7	–3.0	–8.9	–8.1	–7.6	–7.3
5. $[\text{Mg W}_6]^{2+} + (\text{a-b-a})^{2-}$	$[\text{Mg W}_5 (\text{A-b-a})]^0$			–389.3 ^b	–104.8	–58.4	–27.5	–16.2
6. $[\text{Mg W}_5 (\text{A-b-a})]^0$	$[\text{Mg W}_4 (\text{A-b-A})]^0$	4.6 (5.4) ^c	11.7 (10.7) ^c	–7.1 (–5.3) ^c	–11.9 (–10.5) ^c	–10.8 (–9.6) ^c	–10.0 (–9.1) ^c	–9.7 (–8.9) ^c
7. $[\text{Mg W}_4 (\text{A-b-A})]^0$	$[\text{Mg W}_3 (\text{A-B-A})]^0$	10.1	9.3	0.8	–6.0	–6.5	–6.9	–7.1

^a ΔG^2 , ΔG^4 , ΔG^{10} , and ΔG^{20} denote ligand exchange free energies in a protein binding cavity with increasing degree of solvent exposure; upper-case letters denote the ligating group (carboxylic, A, or amide, B) from the model protein ligand that is bound to Mg^{2+} . ^b Approximated as $\Delta G^1 \approx \Delta E_{\text{elec}}$ (see text). ^c Calculated for complexes with model protein ligands comprising two six-methylene spacers, $^-\text{OOC}-(\text{CH}_2)_6-\text{CH}(\text{CONH}_2)-(\text{CH}_2)_6-\text{COO}^-$.

were computed. To mimic such a rigid cavity, the metal-free protein ligand structure (Figure 1a, left) was taken from the “folded” metal complex (Figure 1a, right) by omitting the Mg^{2+} and water molecules. Thus, the gas-phase free energy for the first water exchange in Table 2 was approximated by $\Delta G^1 \approx \Delta E_{\text{elec}}$. The protein ligating groups that directly coordinate to Mg^{2+} are denoted by upper-case letters in Table 2, while those that are *not* bound to the metal ion remain in lower-case letters.

In successively replacing Mg^{2+} -bound water molecules with protein ligands, the first water \rightarrow carboxylate exchange in a fully or partially buried protein cavity is the most favorable for both types of model protein ligands (Table 2, ΔG^x for reactions 1 and 5 are more negative than those for the other reactions). Moreover, a higher negative charge of the protein cavity favors the first water \rightarrow carboxylate exchange (Table 2, the ΔG^x for reaction 5 are more negative than the respective ΔG^x for reaction 1). This is because in a relatively buried cavity, the attractive electrostatic interactions between the oppositely charged ions increase with increasing net charge of the model protein ligand. Increasing solvent exposure of the metal-binding cavity decreases the absolute exchange free energies mainly because the desolvation penalty of the incoming $[\text{Mg W}_6]^{2+}$ complex is greater than the solvation free energy gain in releasing a water molecule from the protein cavity into bulk solution. Nevertheless, the exchange free energies remain negative even for a partially buried cavity.

As compared to the first water \rightarrow carboxylate exchange, the second water substitution is thermodynamically less favorable, irrespective of the nature (carboxylate or carbonyl group) of the model protein ligand (Table 2, ΔG^x for reactions 2 or 3, and 6 are less negative than those for reactions 1 and 5, respectively). Interestingly, once a carboxylate group binds Mg^{2+} and reduces its net positive charge, replacing another Mg^{2+} -bound water molecule is *enthalpically* unfavorable (Table 2, positive ΔH^\dagger for reactions 2, 3, and 6). Instead, the second water substitution is driven by (i) the liberation of a metal-bound water molecule (Table 2, positive $T\Delta S^\dagger$ for reactions 2, 3, and 6) and (ii) the solvation free energy gain as it escapes from the metal-binding site ($\epsilon = 2, 4, 10$, or 20) into bulk solution ($\epsilon = 80$). In the case of the (a–b–b)[–] protein cavity, once Mg^{2+} is bound by a carboxylate group, it prefers to bind to the terminal carbonyl oxygen rather than the central carbonyl one (Table 2, ΔG^x for reaction 3 are more negative than those for reaction 2).

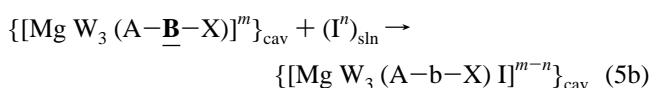
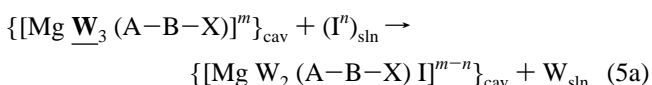
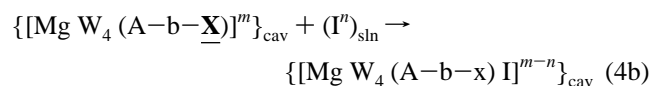
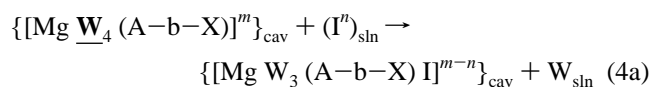
The third water substitution is even less favorable than the previous two (Table 2, ΔG^x for reactions 4 and 7 are less negative than those for the other reactions). This is probably because the charge-accepting ability of Mg^{2+} has been greatly diminished by charge transfer from the first two ligating groups

to the metal ion.^{17,61} Thus, as for the second water substitution, it is mainly the freeing of a metal-bound water molecule and its subsequent hydration that renders the third water \rightarrow amide exchange favorable in the protein (Table 2, negative ΔG^x , $x = 2$ – 20 , for reactions 4 and 7).

Altering the length of the polymethylene spacers between the carboxylate and the carbonyl groups in the model ligands do not affect the trends in ΔG found above. Thus, replacing the $-(\text{CH}_2)_5-$ spacer between *b* and *a* in the (a–b–a)^{2–} ligand by $-(\text{CH}_2)_6-$ decreases the absolute ΔG^x ($x = 2$ – 20) by ~ 1 kcal/mol, but it does not change the sign of any of the thermodynamical parameters (Table 2, reaction 6, values in parentheses).

In summary, the results in Table 2 show that the successive binding of hydrated Mg^{2+} to one or two carboxylate side chains and carbonyl groups in a fully or partially buried protein cavity is thermodynamically favorable (Table 2, negative ΔG^2 , ΔG^4 , ΔG^{10} , and ΔG^{20}).

Competition Between Cellular Ions and Protein Ligands for Bound Mg^{2+} . Although inorganic anions such as Cl^- , H_2PO_4^- , and SO_4^{2-} cannot bind directly to Mg^{2+} in the intracellular space (see above and Table 1), can they compete for the metal ion once Mg^{2+} is bound to amino acid residues in a protein cavity? In other words, can Cl^- , H_2PO_4^- , and SO_4^{2-} anions disrupt the native metal-binding site by displacing some of the metal-bound ligands? To answer this question, we evaluated the free energies for replacing a metal-bound water molecule (W) or protein-ligating group (X = a carboxylic group, A, or an amide group, B) with an inorganic ligand ($\text{I}^- = \text{Cl}^-$, H_2PO_4^- , or SO_4^{2-}) coming from bulk solvent:



As for the stepwise binding of Mg^{2+} to the two model protein ligands, (a–b–b)[–] and (a–b–a)^{2–}, protein ligating groups that are directly metal-bound are highlighted by upper-case letters, while those that are not metal-bound remain as lower case-

Table 3. Calculated Free Energies for Exchanging a Mg^{2+} -Bound Ligand for an Inorganic Anion in Model Mg^{2+} -Binding Sites of Varying Solvent Exposure (in kcal/mol)^a

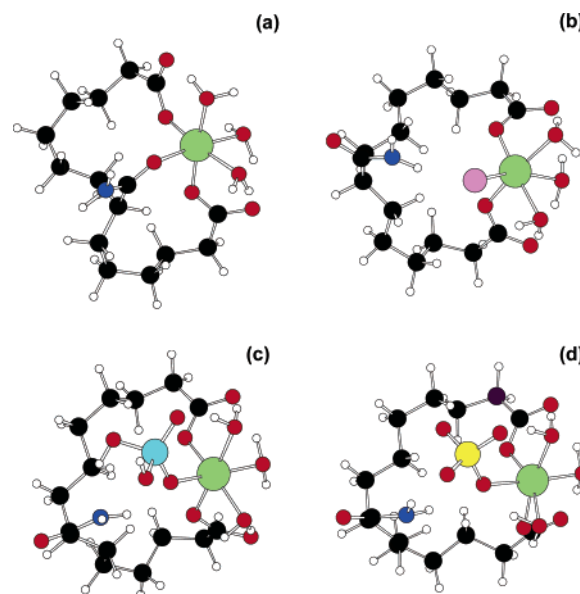
Reactants	Products	ΔG^1	ΔG^2	ΔG^4	ΔG^{10}	ΔG^{20}
1. $[\text{Mg } \underline{\text{W}}_4 (\text{A}-\text{b}-\text{A})]^0 + \text{Cl}^-$	$[\text{Mg } \text{W}_3 (\text{A}-\text{b}-\text{A}) \text{Cl}]^- + \text{W}$	-18.1	30.3	19.0	12.0	9.6
2. $[\text{Mg } \text{W}_4 (\text{A}-\text{b}-\text{A})]^0 + \text{Cl}^-$	$[\text{Mg } \text{W}_4 (\text{A}-\text{b}-\text{a}) \text{Cl}]^-$	-12.4	42.9	31.4	24.0	21.4
3. $[\text{Mg } \text{W}_4 (\text{A}-\text{b}-\text{A})]^0 + \text{H}_2\text{PO}_4^-$	$[\text{Mg } \text{W}_4 (\text{A}-\text{b}-\text{a}) \text{H}_2\text{PO}_4]^-$	-6.4	76.0	62.5	52.2	47.8
4. $[\text{Mg } \text{W}_4 (\text{A}-\text{b}-\text{A})]^0 + \text{H}_2\text{PO}_4^-$	$[\text{Mg } \text{W}_3 (\text{A}-\text{b}-\text{a}) \text{H}_2\text{PO}_4]^- + \text{W}$	-5.9	67.3	52.8	43.0	39.4
5. $[\text{Mg } \text{W}_4 (\text{A}-\text{b}-\text{A})]^0 + \text{SO}_4^{2-}$	$[\text{Mg } \text{W}_4 (\text{A}-\text{b}-\text{a}) \text{SO}_4]^{2-}$	-51.0	126.6	88.8	64.7	56.2
6. $[\text{Mg } \underline{\text{W}}_3 (\text{A}-\text{B}-\text{A})]^0 + \text{Cl}^-$	$[\text{Mg } \text{W}_2 (\text{A}-\text{B}-\text{A}) \text{Cl}]^- + \text{W}$	-29.0	22.5	13.1	7.3	5.4
7. $[\text{Mg } \underline{\text{W}}_3 (\text{A}-\text{B}-\text{A})]^0 + \text{H}_2\text{PO}_4^-$	$[\text{Mg } \text{W}_2 (\text{A}-\text{B}-\text{A}) \text{H}_2\text{PO}_4]^- + \text{W}$	-16.1	59.0	45.2	34.7	30.3
8. $[\text{Mg } \underline{\text{W}}_3 (\text{A}-\text{B}-\text{A})]^0 + \text{SO}_4^{2-}$	$[\text{Mg } \text{W}_2 (\text{A}-\text{B}-\text{A}) \text{SO}_4]^{2-} + \text{W}$	-76.5	93.3	55.4	31.5	23.3
9. $[\text{Mg } \text{W}_3 (\text{A}-\underline{\text{B}}-\text{A})]^0 + \text{Cl}^-$	$[\text{Mg } \text{W}_3 (\text{A}-\text{b}-\text{A}) \text{Cl}]^-$	-30.3	29.9	21.3	16.6	15.2
10. $[\text{Mg } \text{W}_3 (\text{A}-\underline{\text{B}}-\text{A})]^0 + \text{H}_2\text{PO}_4^-$	$[\text{Mg } \text{W}_3 (\text{A}-\text{b}-\text{A}) \text{H}_2\text{PO}_4]^-$	-22.4	61.1	48.7	39.5	35.9
11. $[\text{Mg } \text{W}_3 (\text{A}-\underline{\text{B}}-\text{A})]^0 + \text{H}_2\text{PO}_4^-$	$[\text{Mg } \text{W}_2 (\text{A}-\text{b}-\text{A}) \text{H}_2\text{PO}_4]^- + \text{W}$	-27.1	49.7	36.9	27.4	23.5
12. $[\text{Mg } \text{W}_3 (\text{A}-\underline{\text{B}}-\text{A})]^0 + \text{SO}_4^{2-}$	$[\text{Mg } \text{W}_3 (\text{A}-\text{b}-\text{A}) \text{SO}_4]^{2-}$	-87.1	94.2	59.7	38.3	30.9
13. $[\text{Mg } \underline{\text{W}}_4 (\text{A}-\text{b}-\text{B})]^+ + \text{Cl}^-$	$[\text{Mg } \text{W}_3 (\text{A}-\text{b}-\text{B}) \text{Cl}]^0 + \text{W}$	-98.6	-15.1	-8.3	-4.4	-3.2
14. $[\text{Mg } \text{W}_4 (\text{A}-\text{b}-\text{B})]^+ + \text{Cl}^-$	$[\text{Mg } \text{W}_4 (\text{A}-\text{b}-\text{b}) \text{Cl}]^0$	-77.2	12.3	18.8	22.6	23.7
15. $[\text{Mg } \text{W}_4 (\text{A}-\text{b}-\text{B})]^+ + \text{H}_2\text{PO}_4^-$	$[\text{Mg } \text{W}_4 (\text{A}-\text{b}-\text{b}) \text{H}_2\text{PO}_4]^0$	-73.9	40.0	43.4	44.4	44.4
16. $[\text{Mg } \text{W}_4 (\text{A}-\text{b}-\text{B})]^+ + \text{SO}_4^{2-}$	$[\text{Mg } \text{W}_4 (\text{A}-\text{b}-\text{b}) \text{SO}_4]^-$	-195.1	46.6	41.6	37.3	35.4
17. $[\text{Mg } \underline{\text{W}}_3 (\text{A}-\text{B}-\text{B})]^+ + \text{Cl}^-$	$[\text{Mg } \text{W}_2 (\text{A}-\text{B}-\text{B}) \text{Cl}]^0 + \text{W}$	-99.4	-14.6	-7.1	-2.7	-1.3
18. $[\text{Mg } \text{W}_3 (\text{A}-\text{B}-\text{B})]^+ + \text{Cl}^-$	$[\text{Mg } \text{W}_3 (\text{A}-\text{b}-\text{B}) \text{Cl}]^0$	-88.6	0.2	6.0	9.1	10.1
19. $[\text{Mg } \text{W}_3 (\text{A}-\underline{\text{B}}-\text{B})]^+ + \text{H}_2\text{PO}_4^-$	$[\text{Mg } \text{W}_3 (\text{A}-\text{b}-\text{B}) \text{H}_2\text{PO}_4]^0$	-78.5	31.9	31.3	27.6	25.0
20. $[\text{Mg } \text{W}_3 (\text{A}-\underline{\text{B}}-\text{B})]^+ + \text{SO}_4^{2-}$	$[\text{Mg } \text{W}_3 (\text{A}-\text{b}-\text{B}) \text{SO}_4]^-$	-199.6	42.3	37.6	33.6	31.9
21. $[\text{Mg } \underline{\text{W}}_4 (\text{B}-\text{b}-\text{B})]^{2+} + \text{Cl}^-$	$[\text{Mg } \text{W}_3 (\text{B}-\text{b}-\text{B}) \text{Cl}]^+ + \text{W}$	-159.3	-43.1	-19.7	-5.4	-0.7
22. $[\text{Mg } \text{W}_4 (\text{B}-\text{b}-\text{B})]^{2+} + \text{Cl}^-$	$[\text{Mg } \text{W}_4 (\text{B}-\text{b}-\text{b}) \text{Cl}]^+$	-145.3	-21.1	3.1	17.7	22.6
23. $[\text{Mg } \underline{\text{W}}_3 (\text{B}-\text{B}-\text{B})]^{2+} + \text{Cl}^-$	$[\text{Mg } \text{W}_2 (\text{B}-\text{B}-\text{B}) \text{Cl}]^+ + \text{W}$	-167.9	-51.1	-27.3	-13.0	-8.1
24. $[\text{Mg } \text{W}_3 (\text{B}-\underline{\text{B}}-\text{B})]^{2+} + \text{Cl}^-$	$[\text{Mg } \text{W}_3 (\text{B}-\text{b}-\text{B}) \text{Cl}]^+$	-147.7	-31.5	-12.5	-1.9	1.5

^a Superscripts 2, 4, 10, and 20 denote a metal-binding cavity with increasing solvent exposure; upper-case letters represent carboxylic (A) or amide (B) ligating groups from the model protein ligand that are bound to Mg^{2+} ; lower-case letters represent carboxylic (a) or amide (b) ligating groups from the model protein ligand that are not directly bound to Mg^{2+} ; underlined letters represent metal-bound ligands that are displaced by the inorganic ions; H_2PO_4^- denotes dihydrogen phosphate bidentately bound to Mg^{2+} .

letters. In eqs 4 and 5, $m = 0, 1$, or 2, the subscript “cav” indicates a protein cavity characterized by a dielectric constant of 2, 4, 10, or 20, the subscript “sln” denotes aqueous solution, and the underlined letters highlight the metal-bound ligand that is displaced. The displaced carboxylate or amide group becomes part of the second coordination sphere and is bound to Mg^{2+} in an *outer-sphere* mode (Figure 2), whereas any displaced water molecules are assumed to eventually escape into bulk solution. The free energies evaluated for eqs 4 and 5 are listed in Table 3.

Dependence on the Attacking Anion. In a protein cavity, whether a cellular anion could displace a Mg^{2+} -bound ligand depends mainly on its hydration free energy. The smaller the absolute hydration free energy of the anion, the smaller its desolvation penalty in coming from bulk solution ($\epsilon = 80$) into a protein cavity ($\epsilon \leq 20$), and hence the more likely the anion could displace a weakly bound protein ligand. This is evidenced by the fact that Cl^- , which has the smallest absolute hydration free energy and hence least desolvation penalty among the three anions (see Table 1 footnote b), has the smallest $|\Delta G^x|$ ($x = 2-20$) among the respective reactions involving different anions. For example, the ΔG^4 free energies for displacing a Mg^{2+} -bound water molecule in $[\text{Mg } \text{W}_3 (\text{A}-\text{B}-\text{A})]^0$ with Cl^- , H_2PO_4^- , and SO_4^{2-} are 13, 45, and 55 kcal/mol, respectively (Table 3, reactions 6–8).

The oxyanion binding mode to the metal cation does not seem to determine if it could bind a metal cation in a protein. Although the *bidentate* mode is favored over the *monodentate* mode

**Figure 2.** Ball-and-stick diagrams of fully optimized structures of (a) $[\text{Mg } (\text{H}_2\text{O})_3 (\text{A}-\text{B}-\text{A})]^0$, (b) $[\text{Mg } (\text{H}_2\text{O})_3 \text{Cl} (\text{A}-\text{b}-\text{A})]^-$, (c) $[\text{Mg } (\text{H}_2\text{O})_3 (\text{H}_2\text{-PO}_4) (\text{A}-\text{b}-\text{A})]^-$, and (d) $[\text{Mg } (\text{H}_2\text{O})_3 (\text{SO}_4) (\text{A}-\text{b}-\text{A})]^{2-}$.

(mainly because of the additional free energy gain upon releasing an additional water molecule from the cavity to bulk solution), it does not change the thermodynamic outcome of the protein ligand \rightarrow anion exchange (Table 3, reactions 3 and 4, or 10 and 11; positive ΔG^x , $x = 2-20$, for phosphate both monodentately and bidentately bound to Mg^{2+}).

Dependence on the Nature of the Metal-Bound Ligand: Carboxylates/Amides vs Water. The results in Table 3 show that a metal-bound water molecule is more vulnerable to an “alien” anion attack than a metal-bound carboxylate/amide

- (59) Ben-Naim, A.; Marcus, Y. *J. Chem. Phys.* **1984**, *81* (4), 2016–2027.
 (60) Friedman, H. L.; Krishnan, C. V., Thermodynamics of ionic hydration. In *Water: A comprehensive treatise*, Franks, F., Ed. Plenum Press: New York, 1973; Vol. 3, pp 1–118.
 (61) Dudev, T.; Lim, C. *J. Phys. Chem. A* **1999**, *103*, 8093–8100.

because it binds less tightly to Mg^{2+} than the latter.^{21,61} In a fully or partially buried (a–b–a)^{2–} or (a–b–b)[–] cavity, displacing a Mg^{2+} -bound protein ligand (carboxylate or amide) by an inorganic anion is thermodynamically unfavorable regardless of whether the anion binds monodentately or bidentately to the metal ion (positive ΔG^x , $x = 2-20$, for reactions 2–5, 9–12, 14–16, and 18–20). However, in a monoanionic (a–b–b)[–] or neutral (b–b–b)⁰ cavity where electrostatic interactions with the metal cation are weaker than those in a dianionic (a–b–a)^{2–} cavity, displacing the more weakly bound water molecule becomes thermodynamically favorable (Table 3, negative ΔG^x for reactions 13, 17, 21, and 23). This implies that an inorganic anion from the intracellular fluids cannot displace a Mg^{2+} -bound protein residue, but it could replace a Mg^{2+} -bound water in a monoanionic or neutral protein cavity.

Dependence on the Protein Cavity. The likelihood of a given anion disrupting a native Mg^{2+} -binding site depends largely on (1) the number of metal-bound carboxylates (which in turn determines the overall charge of the protein cavity) and (2) the solvent exposure of the metal-binding site. In the absence of metal-bound carboxylates, decreasing the solvent exposure of the metal-binding site enhances the charge–charge interactions between the dicationic Mg^{2+} complex and the incoming anion. This could suffice to compensate for the desolvation penalty of the incoming Cl^- , enabling the anion to displace a weakly bound neutral ligand. Thus, when Mg^{2+} binds to two or three amide groups in a buried cavity to form a dicationic $[\text{Mg W}_4 (\text{B–b–B})]^{2+}$ or $[\text{Mg W}_3 (\text{B–B–B})]^{2+}$ complex, respectively, a chloride could displace a metal-bound water or amide group (Table 3, negative ΔG^2 for reactions 21–24).

In summary, increasing the number of metal-bound carboxylates increases the protection level of the binding site against attacks from the intracellular anions. Thus, while in a neutral (b–b–b)⁰ buried cavity Cl^- can displace both amide and water ligands from the metal's first coordination shell (Table 3, negative ΔG^2 for reactions 21–24), it can displace only Mg^{2+} -bound water in an anionic (a–b–b)[–] binding site (Table 3, negative ΔG^x , $x = 2-20$, for reactions 13 and 17), but none of the Mg^{2+} -bound ligands in a dianionic (a–b–a)^{2–} cavity (Table 3, positive ΔG^x , $x = 2-20$, for reactions 1–12).

PDB Survey. Our PDB search produced only four X-ray structures of Mg^{2+} -binding sites in proteins containing inorganic anions of interest in this work. These are 1L7M (phosphoserine phosphatase), 1Q91 (deoxyribonucleotidase), 1RMW (acid phosphatase/phosphotransferase), which contain a phosphate group monodentately bound to Mg^{2+} , and 1YMQ (sugar phosphatase), which contains a sulfate anion also monodentately bound to the metal cofactor. All these binding sites are deeply buried (the solvent accessible surface area of the metal-bound protein residues range from 3% to 16%) and belong to the (a–b–a)^{2–} type where two Asp residues and one backbone peptide group coordinate to the metal ion (see Discussion).

Discussion

Comparison with Available Experimental Data. The finding that Mg^{2+} and cellular inorganic anions remain as solvent-separated ion pairs in the cytoplasmic solution (Table 1, positive ΔG^{80}) is consistent with the respective experimental data that is currently available. The free energy for $\text{Mg}^{2+} + \text{Cl}^- \rightarrow [\text{MgCl}]^+$ varies from 0.1 to 1.4 kcal/mol in aqueous solution,

implying that inner-shell binding of Cl^- to Mg^{2+} is thermodynamically unfavorable.⁶² Analogous reactions between Cl^- and other cations such as Na^+ , Ca^{2+} , Sr^{2+} , Ba^{2+} and lanthanide trications are also thermodynamically unfavorable with positive solution free energies.⁶²

The finding that in a fully or partially buried protein cavity, Mg^{2+} can bind to either one Asp/Glu side chain and two backbone or side-chain carbonyl oxygen atoms or two Asp/Glu side chains and a carbonyl group (Table 2, negative ΔG^x , $x = 2-20$) is supported by PDB structures of Mg^{2+} -bound proteins:¹⁷ Mg^{2+} is bound to one Asp/Glu side chain and two backbone or side-chain carbonyl oxygen atoms in ~6% of the Mg^{2+} -binding sites, while it is bound to two Asp/Glu side chains and a neutral protein group in ~19% of the Mg^{2+} -binding sites.¹⁷

The calculations predict that an inorganic intracellular anion cannot displace a Mg^{2+} -bound carboxylate or amide group (Table 3). Indeed, for each of the four X-ray structures containing a Mg^{2+} -bound phosphate or sulfate group (1L7M, 1Q91, 1RMW, and 1YMQ; see Results), there exists a counterpart structure without phosphate or sulfate (1NNL, 1Q92, 1N9K, and 1RKQ, respectively), in which Mg^{2+} is bound to the same set of protein ligands (two Asp side chains and one backbone amide group) and three water molecules. This suggests that the phosphate or sulfate anion did not displace any of the Mg^{2+} -bound protein ligands, but rather, it replaced a Mg^{2+} -bound water molecule.

The observation that a Mg^{2+} -bound water in a dianionic (a–b–a)^{2–} buried cavity has been replaced by a phosphate (PDB entry 1L7M, 1Q91, and 1RMW) or a sulfate (PDB entry 1YMQ) seems to be at odds with our calculations suggesting that substituting a Mg^{2+} -bound water in this type of cavity with an inorganic anion is thermodynamically unfavorable (Table 3; positive ΔG^x , $x = 2-20$, for reactions 6–8). Note, however, that the protein crystals for the four X-ray structures, 1L7M, 1Q91, 1RMW, and 1YMQ, have been purified/crystallized in the presence of 50 to 200 mM of the respective anion.^{63–66} Such a great excess of the phosphate/sulfate anion promotes its binding to the metal cation. Moreover, all four X-ray structures, 1L7M, 1Q91, 1RMW, and 1YMQ, contain a positively charged lysine and/or arginine residue in the metal's second coordination sphere that partially neutralizes the negative charge of the dianionic protein cavity, enabling thus water \rightarrow inorganic anion exchange (see **Dependence on the Protein Cavity** in the Results section).

Why Does the Metal Ion Prefer Binding to Protein Rather than Inorganic Ligands? The results in Tables 1 and 2 show that Mg^{2+} will not exchange its first-shell water molecules for inorganic anions present in the aqueous environment of the cell, but it could exchange some (but not all) of its first-shell water molecules for Asp/Glu carboxylates as well as backbone/side-chain amides in a buried/partially buried protein cavity. Two factors mainly contribute to the observed preference of a metal cation for negatively charged amino acid (rather than nonprotein)

(62) Martell, A. E. *Critical Stability Constants*. Plenum Press: 1984.

(63) Lu, Z.; Dunaway-Mariano, D.; Allen, K. N. *Biochemistry* **2005**, *44*, 8684–8696.

(64) Rinaldo-Matthis, A.; Rampazzo, C.; Balzarini, J.; Reichard, P.; Bianchi, V.; Nordlund, P. *Mol. Pharmacol.* **2004**, *65*, 860–867.

(65) Wang, W.; Cho, H. S.; Kim, R.; Jancarik, J.; Yokota, H.; Nguyen, H. H.; Grigoriev, I. V.; Wemmer, D. E.; Kim, S.-H. *J. Mol. Biol.* **2002**, *319*, 421–431.

(66) Calderone, V.; Forleo, C.; Benvenuti, M.; Thaller, M. C.; Rossolini, G. M.; Mangani, S. *J. Mol. Biol.* **2006**, *355*, 708–721.

ligands. The first factor is the reduced cost of desolvating the negatively charged Asp/Glu carboxylate groups in a protein cavity, as opposed to the much higher penalty of desolvating an inorganic anion in aqueous solution. The second factor is the chelating effect of the binding site, which acts as a polydentate ligand that employs all its ligating entities to bind the metal cation. As illustrated in Figure 1a for the polydentate $(a-b-A)^{2-}$ protein ligand, one of the carboxylate groups dislodges a Mg^{2+} -bound water molecule and binds to the metal ion, while the other carboxylate group and amide oxygen form hydrogen bonds with the first-shell water molecules; thus the ΔG^1 for water $\rightarrow (a-b-A)^{2-}$ exchange (Table 2, reaction 5) is more favorable than that for water $\rightarrow SO_4^{2-}$ (Table 1, reaction 4 or 5). Hence, the protein cavity and its interactions help to sequester the metal ion from the surrounding fluids.

Factors Governing the Competition Between Protein and Inorganic Ligands for the Metal Cation. Hydration Free Energy of the Cellular Anion. The charge of the anion has opposing effects on the metal ligand \rightarrow anion substitution. In a solvent-inaccessible cavity, dianions such as SO_4^{2-} are more efficient ligating entities than monoanions such as $H_2PO_4^-$ due to the increased charge–charge interactions with the metal cation. On the other hand, dianions have to pay a much greater desolvation penalty than their monoanionic counterparts in entering a buried protein cavity, which generally outweighs the favorable metal–anion interactions, as evidenced by the finding that dianions generally have more unfavorable ligand exchange free energies than the monoanions (Table 3). Hence, the smaller the absolute hydration free energy of a cellular anion, the more likely a cellular anion could compete with weakly bound neutral ligands for the metal cation in a protein cavity.

Overall Charge of the Protein Cavity. The greater the net negative charge of the protein cavity, the less vulnerable the metal-binding site is prone to attack by “alien” inorganic ligands. In a fully or partially buried dianionic cavity, an intracellular anion may not displace any of the Mg^{2+} -bound ligands, as evidenced by the positive ΔG^x ($x = 2-20$) in the neutral $[Mg W_4 (A-b-A)]^0$ and $[Mg W_3 (A-B-A)]^0$ complexes (Table 3, reactions 1 and 12). However, when the net negative charge of the protein cavity is reduced from -2 to -1 by the presence of only one carboxylate group or positively charged residues in the metal’s second coordination shell, a Cl^- may displace the more weakly bound water, as evidenced by the negative ΔG^x ($x = 2-20$) for water \rightarrow chloride exchange in the monocationic $[Mg W_4 (A-b-B)]^+$ and $[Mg W_3 (A-B-B)]^+$ complexes (Table 3, reactions 13 and 17) and in the four X-ray structures containing a Mg^{2+} -bound phosphate or sulfate group (1L7M, 1Q91, 1RMW, and 1YMQ). In a buried neutral protein cavity, a Cl^- may not only displace a water molecule, but also an amide group from Mg^{2+} , as evidenced by the negative ΔG^2 for water/amide \rightarrow chloride exchange in the dicationic $[Mg W_4$

$(B-b-B)]^{2+}$ and $[Mg W_3 (B-B-B)]^{2+}$ complexes (Table 3, reactions 21–24).

Solvent Accessibility of the Binding Site. The relative solvent exposure of the metal-binding site has opposite effects, depending on the net charge of the metal complex. For dicationic metal complexes, decreasing solvent exposure favors water/amide \rightarrow chloride exchange as the favorable charge–charge interactions between the dication and the anion could outweigh the desolvation penalty of the incoming anion (Table 3, reactions 21–24). On the other hand, for neutral metal complexes, increasing solvent exposure makes the water/amide \rightarrow anion exchange less unfavorable as the anion-substituted metal complex is better solvated than the native metal complex; however, this is not sufficient to fully compensate for the desolvation penalty of the incoming anion.

How Does the Metal-Binding Site Defend Itself from Alien Attack by Cellular Anions That May Disrupt the Native Binding-Site Geometry? Increasing the net negative charge of the protein cavity, while decreasing the number of available amide groups for metal binding, protects the Mg^{2+} -bound ligands from being displaced by alien anions. A highly negatively charged metal-binding cavity appears to be more effective in repelling attacks from “alien” anions than a less negatively charged cavity lined with fewer or no negatively charged Asp/Glu residues (Table 3, compare reactions 1–12 with 13–24) and/or containing positively charged Lys/Arg residues in the metal’s second-shell. These results reveal a “novel” role for carboxylate groups in a protein cavity: they not only contribute to the high affinity binding of the metal cation,^{3,21,22,24,25,38} but they also play a protective role against interactions with unwanted species from the cellular fluids. This may explain the fact that functional Mg^{2+} -binding sites with no negatively charged Asp or Glu side chains are not found in the PDB.¹⁷ Such buried sites, lined only by neutral protein ligands, would not only have poor binding affinity for the metal cation, but they would also be quite vulnerable to external anionic attacks (see Table 3, reactions 22 and 24).

Acknowledgment. We are grateful to Drs. D. Bashford, M. Sommer, and M. Karplus for the program to solve the Poisson equation. This work was supported by the National Science Council, Taiwan (NSC Contract No. 91-2311-B-001), the Institute of Biomedical Sciences, and the National Center for High-Performance Computing, Taiwan.

Supporting Information Available: Calibration of gas-phase calculations, solvation free energy calculations, complete ref 50, and structures of Mg^{2+} -inorganic ion complexes. This material is available free of charge via the Internet at <http://pubs.acs.org>.

JA063111S